Journal of Engineering Mathematics **42:** 23–44, 2002.

Boundary-layer behaviour in a hydraulic theory of horizontal oil wells

R. M. S. M. SCHULKES and A. C. KING[1]
Norsk Hydro a.s.a., Research Centre Porsgrunn, N-3901 Porsgrunn, Norway
[1]*School of Mathematics, University of Birmingham, Edgbaston, Birmingham, UK*

Received 11 September 2000; accepted in revised form 21 June 2001

Abstract. In many cases, modern oil production occurs by means of long, more or less horizontally drilled cavities in an oil reservoir, so-called *horizontal wells*. Oil production by means of these horizontal wells is usually advantageous because the contact area between the well and the reservoir can be increased significantly, in particular for oil reservoirs with large aspects ratios. However, it turns out that the production profile along the length of a horizontal well may have boundary-layer-like characteristics with the consequence that a large fraction of the production comes from a small section of the well. In this paper the boundary-layer characteristics of the production profile are analysed. It is shown that different boundary layers with different characteristics can occur simultaneously. In particular it is shown that there may be a thin 'annulus-induced' boundary layer and a thick 'reservoir-induced' boundary-layer.

Key words: boundary layer, horizontal well, hydraulic theory, oil wells

1. Introduction

In many parts of the world *e.g.* the North Sea, oil reservoirs occur predominantly in pancake-like structures where the thickness of the oil layer is small in comparison with the horizontal dimensions of the oil reserve. Recovering oil from such layered structures was not economical until fairly recently, because with conventional (vertical) wells only a small part of the oil reserves can be recovered. The reason for this is that with a vertical well (which can be viewed as a vertical line source) the contact area between the well and the reservoir is bounded by the thickness of the oi llayer. When, as is fairly common, there is an aquifer below and/or a gas-cap above the oil layer, producing oil by means of a vertical well may lead to a fairly rapid advance of the oil-water and/or oil-gas interface towards the well. This phenomenon, called coning, is fairly well understood in homogeneous reservoirs, see *e.g.* Hocking and Forbes [1] among others. In non-homogeneous reservoirs (a situation one always has in practice) the formation of water or gas cones is not easy to predict but may have enormous consequences for the amount of oil which is eventually recovered.

In the early 1990's new drilling techniques made is possible to direct the drill such that it follows the oil layer. With this technique it is nowadays possible to construct long, so-called *horizontal wells*. These wells have a much larger contact area between the well and the reservoir such that it has become possible to produce oil economically from reservoirs where the oil-column has a height down to 10 m. In order to get to the oil-containing structure in the reservoir, one drills downwards until the oil layer is reached, after which the oil-producing well is drilled more or less horizontally. The special foot-like geometry of such a well has lead to the terminology where the closed end of the well is referred to as the *toe* of the well, while

the end of the well which is connected to the vertical (non-producing) part is referred to as the *heel* of the well.

While horizontal wells are extremely successful in increasing the recoverable volume of oil, there are special problems related to oil production by means of such wells. One of the main problems concerns pressure variations along the length of the well. If one imagines a well which produces oil over a length of 1500−2000 m it is clear that the volume flow rate of oil increases monotonically from the toe to the heel of the well. Fairly large fluid velocities can occur in the heel of the well (a velocity up to 5 m/s in the heel is not uncommon) which means that frictional pressure losses in the well can lead to a significant pressure drop along the length of the well. This, in turn, implies that the difference in pressure between the well and the reservoir is not constant along the length of the well. In fact, the pressure difference between the well and the reservoir increases monotonically from the toe towards the heel of the well. Since the rate at which oil is produced locally in a well is proportional to the pressure difference between the well and the reservoir, it follows that oil production is lowest in the toe and increases towards the heel of the well. This increases the likelihood of the formation of gas or water cones near the heel of the well with, often severe, economic consequences.

Horizontal wells in homogeneous reservoirs can be modelled by means of potential theory, provided hydrodynamic pressure losses in the well can be neglected. In those cases the well can be modelled by a line source and closed-from analytical expressions for the productivity of such a well may be obtained, see for example Joshi [2]. Frictional pressure losses in the well have the effect of introducing a nonlinear coupling between the line-source strength and reservoir response. Even for homogeneous reservoirs the well-reservoir coupling quickly becomes so complicated that the problem is only solvable by means of numerical techniques. A way around this problem was presented by Dikken [3]. The well model by Dikken [3] is based on an approximate force balance of the flow in the well and coupling the well to the reservoir by means of a simplified Darcy-like equation. In this approach it is assumed that the local volume flow rate into the well is directly proportional to the pressure difference between the well and the reservoir, assuming a constant reservoir pressure at some given distance from the well. The Dikken-approach is elegant in the sense that one obtains a nonlinear ODE describing the variations in the volume flow rate in the well while the reservoir does no longer appear in the problem. For infinitely long wells Dikken [3] presented analytical solutions to his well equation. Later is was shown by Halvorsen [4] that a simplified form of Dikken's model on a finite domain, retaining the essential nonlinearities, has an analytical solution in terms of a Weierstrass elliptic function. The well-modelling work described above deals with single-phase flow in the well. Although a fair amount of work has been done in the area of multiphase flow well-bore hydraulics (see *e.g.* Ouyang, [5]), the multiphase flow phenomena are so complicated that it becomes exceedingly difficult to gain insight into the well-modelling problem when multiphase flow effects are included.

In the present paper an extension of Dikken's [3] model is discussed retaining the simplification of single-phase flow. The model extension is motivated by the manner in which horizontal wells are constructed in many cases. When a well is drilled in a reservoir which is poorly consolidated (often the case in high- permeability reservoirs), one can not be certain that the bore hole will not collapse. For that reason a perforated steel pipe (called the *base pipe* or the *liner*) is often inserted into the drilled cavity. When the well is in operation, oil will flow in the base pipe as well as in the annular space which may exist on the outside of the base pipe (provided the cavity has not collapsed). Dikken's model essentially assumes that there is no annular space on the outside of the base pipe, resulting in one nonlinear ODE describing

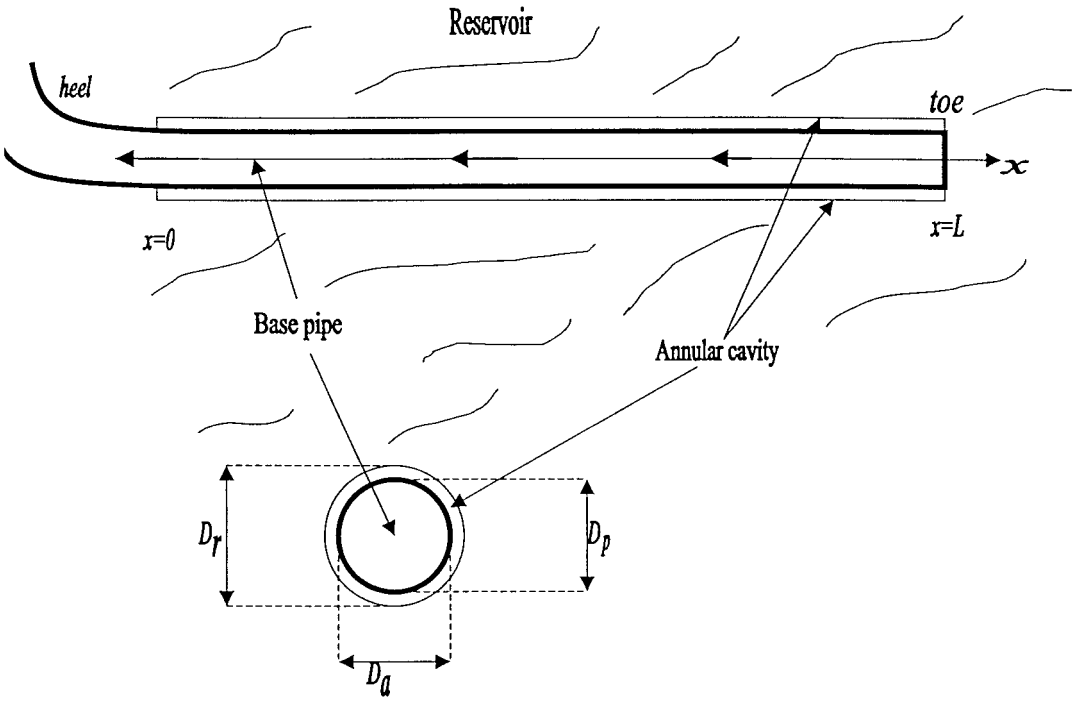

Figure 1. A schematic diagram showing the geometry of the system to be considered.

the flow in the base pipe. When one allows for flow in the annular cavity, two coupled, non linear ODE's are obtained which, as it turns out, have interesting solution characteristics in the form of multiple boundary layers. It is this extension of Dikken's model which will be the subject of the present paper.

2. Governing equations

In this paper we assume that a well with a length L is situated along the positive x-axis. A fluid with a constant density p and viscosity μ flows from the reservoir into the well. The well geometry is as shown in Figure 1. A base pipe with a variable inner diameter equal to D_p is situated in a circular bore hole with a variable inner diameter D_r. The base pipe is not necessarily concentric with the annulus.

The base pipe has a constant outer diameter equal to D_a. Owing to the extreme aspect ratio of the flow problem under consideration, ($D_a/L \sim 10^{-4}$) it is natural to take the hydraulic approach by considering only variations in the x-component of the velocity in the well and the annular cavity. Momentum conservation in the base pipe yields

$$\rho \frac{\mathrm{d}}{\mathrm{d}x}(A_p u_p^2) - \rho \lambda_p \pi D_p u_p v = -A_p \frac{\mathrm{d}p_p}{\mathrm{d}x} - \tau_p \pi D_p \, . \tag{1}$$

in which A_p, u_p, p_p and τ_p denote the cross sectional area, the mean fluid velocity, the pressure and the wall shear stress, respectively. A subscript p always refers to a quantity defined in the base pipe. The second term on the left-hand side of (1) is related to the change in x-momentum resulting from radial flow through the pipe wall. The physical origin of this term is related to the change in the flow structure near the pipe wall due to the radial inflow. This term

has been quantified experimentally in a number of experiments, see *e.g.* Olsen and Eckert [6] and Schulkes *et al.* [7] and the parameter $\lambda_p \approx 0{\cdot}2$ turns out to be related to the friction factor. Assuming a porous pipe wall, we denote by v the radial fluid velocity through the wall. The last term on the right-hand side of (1) denotes the shear stress exerted by the wall of the base pipe on the fluid.

The momentum conservation equation in the annular cavity reads

$$\rho \frac{\mathrm{d}}{\mathrm{d}x}(A_a u_a^2) - \rho\lambda'' \pi D_r u_a w + \rho\lambda' \pi D_a u_a v' - A_a \frac{\mathrm{d}p_a}{\mathrm{d}x} - \tau_a \pi D_a - \tau_r \pi D_r \ . \tag{2}$$

The notation is the same as for the pipe equation with the difference that in the above equation a subscript a always refers to a quantity defined in the annular cavity. The second and third term on the left-hand side of (2) are, as before, related to changes in x-momentum due to radial flow. The term containing λ'' is related to the increase in axial momentum due to inflow from the reservoir, w denoting the radial velocity from the reservoir into the annulus; the term containing λ' describes the decrease in axial momentum due to flow from the annulus into the perforations of the base pipe, v' denoting the radial velocity into the base pipe. The last two terms on the right-hand side of (2) denote shear stresses on the external base pipe wall and bore hole, respectively.

Equations (1) and (2) need to be augmented with mass-conservation equations and a number of auxiliary relations in order to obtain a closed system of equations. Mass conservation in the annular cavity and the base pipe yields

$$q_{ra} = w\pi D_r = \frac{\mathrm{d}}{\mathrm{d}x}(A_a u_a) + \frac{\mathrm{d}}{\mathrm{d}x}(A_p u_p) \ , \tag{3}$$

and

$$q_{ap} = v\pi D_p = \frac{\mathrm{d}}{\mathrm{d}x}(A_p u_P) = v'\pi D_a \ , \tag{4}$$

in which q_{ra} and q_{ap} denote the volume flows per unit length from the reservoir into the annulus and the annulus into the base pipe, respectively. Concerning the shear stresses we make the simplifying assumption that the wall shear stress on the external base pipe wall is the same as the shear stress on the bore hole surface, that is $\tau_a = \tau_r$. In addition we apply the Fanning friction factors in order to express the wall shear stress in terms of the mean velocities in the annulus and the base pipe via

$$\tau_w = \frac{1}{8}\rho f_p(u_p) u_p^2, \quad \text{and} \quad \tau_a = \frac{1}{8}\rho f_a(u_a) u_a^2 \ . \tag{5}$$

The friction factors f_p and f_a are assumed to be of the form

$$f_i(u_i) = \frac{a_i}{|\mathrm{Re}_i|^{b_i}}; \quad i = a, p \ , \tag{6}$$

where the Reynolds numbers Re_p and Re_a in the friction factors as defined above are computed using the hydraulic diameters of the base pipe and the annulus, respectively. It turns out that the region in the base pipe in which the flow can be assumed to be laminar is small, confined to the very last part of the well near the toe. For the base pipe we therefore assume fully turbulent flow in the whole of the pipe and use the Blasius friction factor with $a_p = 0{\cdot}316$ and $b_p = 0{\cdot}25$. In the annulus the friction factor is a function of the eccentricity of the base pipe in the annular cavity. Jonsson and Sparrow [8] have shown experimentally that

for turbulent flow $a_a = 0{\cdot}15 - 0{\cdot}0438e^2$ and $b_a = 0{\cdot}18$ where e denotes the eccentricity. For concentric pipes and turbulent flow one can alternatively use $a_a = 0{\cdot}35$ and $b_a = 0{\cdot}25$, see Idelchik [9].

Finally, two auxiliary relations are required to close the system of equations. The first relation expresses the pressure difference between the annular cavity and the base pipe in terms of the volume flow rate through the perforations in the wall of the base pipe. Assuming that the wall of the base pipe acts as a porous medium, we can use Darcy's equation to show that the volume flow rate through the pipe wall is linearly proportional with the pressure difference between the annulus and the base pipe, giving

$$q_{ap} = \beta(p_a - p_p)\ . \tag{7}$$

While the assumption that the base pipe acts as a porous medium may seem rather extreme, this assumption is in fact reasonable. Namely, it is not uncommon to place a type of filter on the outside of the base pipe in order to prevent sand particles from entering the base pipe. This filter, known as a sand screen, has flow-pressure loss characteristics much like a conventional porous medium. The final relation required is a relation which links the volume flow into the annular cavity to the pressure difference between the annulus and the reservoir. Also here one can use Darcy's equation to obtain

$$q_{ra} = J(p_{res} - p_a)\ , \tag{8}$$

in which p_{res} denotes the reservoir pressure (assumed constant) and the parameter J is often referred to as the productivity index. The reader is referred to standard texts in the field of petroleum technology; see for example Golan and Whitson [10] for a derivation of Equation (8). The productivity index J is proportional to the reservoir permeability and gives a measure of the rate of oil production per unit length, per unit pressure difference between the well and the reservoir.

We now obtain the final equations by using (7) and (8) to eliminate the pressures from the momentum equations while using equations (3)–(5) to express all remaining variables in terms of the annulus and base-pipe velocities. In order to simplify the equations somewhat we now assume that $\lambda' = \lambda'' = \lambda_a$. With these simplifications the following coupled, second-order differential equations are obtained

$$\begin{aligned}&\frac{A_p}{\beta}\frac{\mathrm{d}^2}{\mathrm{d}x^2}(u_pA_p) + \frac{A_p}{J}\left[\frac{\mathrm{d}^2}{\mathrm{d}x^2}(u_pA_p) + \frac{\mathrm{d}^2}{\mathrm{d}x^2}(u_aA_a)\right] - \\ &\rho\frac{\mathrm{d}}{\mathrm{d}x}(A_pu_p^2) + \rho\lambda_pu_p\frac{\mathrm{d}}{\mathrm{d}x}(A_pu_p) - \frac{\pi D_p}{8}f_pu_p^2 = 0,\end{aligned} \tag{9}$$

$$\begin{aligned}&\frac{A_a}{J}\frac{\mathrm{d}^2}{\mathrm{d}x^2}(u_pA_p) + \frac{A_a}{J}\frac{\mathrm{d}^2}{\mathrm{d}x^2}(u_aA_a) - \rho\frac{\mathrm{d}}{\mathrm{d}x}(A_au_a^2) + \\ &\rho\lambda_au_a\frac{\mathrm{d}}{\mathrm{d}x}(A_au_a) - \frac{\rho\pi(D_a + D_0)}{8}f_au_a^2 = 0.\end{aligned} \tag{10}$$

The boundary conditions for the equations are as follows. The annulus is blocked in both the heel and the toe of the well, giving

$$u_a(0) = u_a(L) = 0\ . \tag{11}$$

In the base pipe we specify the fluid velocities in the heel and the toe, giving

$$U_p(0) = U_o, \quad u_p(L) = 0 \, . \tag{12}$$

One quantity of interest is the pressure difference between the base pipe and the reservoir since it is this pressure difference which determines the rate of oil production in each section of the well. Using (3), (4) and (7), (8) we find that the pressure difference between the base pipe and the reservoir, Δp_{rp}, is given by

$$\Delta p_{rp} = \frac{1}{\beta}\frac{\mathrm{d}}{\mathrm{d}x}(u_p A_p) + \frac{1}{J}\left[\frac{\mathrm{d}}{\mathrm{d}x}(u_p A_p) + \frac{\mathrm{d}}{\mathrm{d}x}(u_a A_a)\right] \, . \tag{13}$$

We should note that in reality one controls the pressure in the heel of the well (or at some position downstream from the heel where a choke valve is situated) to adjust the flow rate. This implies that the Neumann boundary condition (13) where Δp_{rp} is specified in the heel may be a more realistic boundary condition than the Dirichlet condition (12). However, for the purpose of analysis it is convenient to work with the Dirichlet condition.

Experiments (Schulkes *et al.* [7]) show that the parameter λ_p is proportional to the fraction factor f_p. Its seems reasonable to assume that the same relation exists between λ_a and the friction factor f_a, although there is, at present, no experimental evidence to confirm this. In this paper we make the simplifying assumption that λ_p is constant with $\lambda_p = 0{\cdot}2$, which is a reasonable approximation for the case of fully turbulent flow. In addition we assume that $\lambda_p = \lambda_a = \lambda$.

The flow in the annulus and the base pipe is now determined by Equations (9)–(10) subject to the boundary conditions (11)–(12). In order to make the analysis in the following section more transparent we take both the annulus and the base-pipe cross-sectional areas to be constant (although some numerical results are presented later in which the cross-sectional areas are variable). In addition, Equations (9) and (10) will be written in dimensionless form. To this end a velocity scale U is required which is representative for the flow in the well. A number of different velocity scales can be used, but for our purpose it is natural to use the base-pipe velocity in the heel of the well as the relevant velocity scale, thus $U = U_0$. As a relevant length scale we take the length of the well L, also that we can introduce the following dimensionless variables

$$\tilde{x} = \frac{x}{L}, \quad \tilde{u}_p = \frac{u_p}{U}, \quad \tilde{u}_a = \frac{u_a}{U}, \quad \tilde{f}_p = \frac{f_p}{2f_p(U)}, \quad \tilde{f}_a = \frac{f_a}{2f_p(U)}\frac{D_p}{D_a - D_o} \, . \tag{14}$$

With the simplifications as mentioned above, Equations (9) and (10) become in dimensionless form

$$\delta_\beta \tilde{u}_p'' + \delta_J \tilde{u}_p'' + r_A \delta_J \tilde{u}_a'' - (2-\lambda)\epsilon \tilde{u}_p \tilde{u}_p' = \tilde{f}_p \tilde{u}_p^2 \, . \tag{15}$$

$$\delta_J \tilde{u}_p'' + r_A \delta_J \tilde{u}_a'' - (2-\lambda)\epsilon \tilde{u}_a \tilde{u}_a' = \tilde{f}_a \tilde{u}_a^2 \, . \tag{16}$$

The dashes denote derivatives with respect to $\tilde{x}$ and the following dimensionless groups have been introduced. The parameter $\delta_\beta = A_p D_p / \beta \rho L^2 U f_p(U)$ is a measure of the ratio of the force required to get fluid through the sand screen and frictional force in the base pipe. Likewise, the parameter $\delta_J = A_p D_p / J \rho L^2 U f_p(U)$ is a measure of the ratio of the force required to extract fluid from the reservoir and the frictional force in the base pipe. The parameter $\epsilon = D_p / L f_p(U)$ is the ratio of inertial and frictional forces. Finally, $r_A = A_a / A_p$ is the ratio of cross sectional areas of the annulus and the base pipe. The boundary conditions to be used in the analysis are as follows

$$\tilde{u}_p(0) = -1, \quad \tilde{u}_p(1) = 0, \quad \text{and} \quad \tilde{u}_a(0) = \tilde{u}_a(1) = 0 \,. \tag{17}$$

The pressure difference between the reservoir and the well, as given in Equation (13), becomes in dimensionless form

$$\Delta\tilde{p} = \delta_\beta \tilde{u}'_p + \delta_J \tilde{u}'_p + r_A \delta_J \tilde{u}'_a \,, \tag{18}$$

in which $\Delta\tilde{p} = D_p \Delta p_{rp} / \rho U^2 f_p(U) L$.

Before we proceed it is convenient to specify typical values of the physical parameters such that the orders of magnitude of the four dimensionless groups as specified above can be found. In this paper we use the following fairly typical values: $D_p = 0{\cdot}16\text{m}$, $L = 1000\text{m}$, $A_a = 0{\cdot}015\text{m}^2$, $\rho = 800$ kg m^{-3}, $\mu = 1\text{cP}$ and $U = 1{\cdot}5\text{ms}^{-1}$. Employing typical parameter values or a sand screen, we find $\beta \approx 10^{-5}$. The productivity index J ranges in size from 10^{-13} m^3 s^{-1} Pa^{-1} m^{-1} for low-permeability reservoirs and to 10^{-9} m^3 s^{-1} Pa^{-1} m^{-1} for high-permeability reservoirs. Employing these parameter values we obtain the following orders of magnitude for the dimensionless variables:

$$r_a = O(1), \quad \epsilon = O(10^{-3}), \quad \delta_\beta = O(10^{-5}), \quad \delta_J = O(10^{-2}) - O(10^2) \,. \tag{19}$$

3. Analysis of the solution characteristics of the equations

In the following three sections. the solution characteristics of Equations (15)–(17) will be studied. It is beneficial to start the analysis with a study of the simplified problem in which flow in the annular cavity is negligible. Insight in the solution characteristics obtained for this case is helpful when analysing the coupled set of equations.

3.1. Special case: no flow in annulus

The case in which there is no flow in the annulus is obtained when we let $A_a \to 0$ in Equation (10). In this limit, Equations (9) and (10) become decoupled and (10) has the solution $u_a(x) \equiv 0$. The set of Equations (15)–(16) now reduces to

$$\delta\tilde{u}''_p - (2-\lambda)\epsilon\tilde{u}_p\tilde{u}'_p = \tilde{f}_p\tilde{u}_p^2 \,, \tag{20}$$

with the boundary conditions

$$\tilde{u}_p(0) = -1, \tilde{u}_p(1) = 0 \,. \tag{21}$$

In (20) we have introduced the parameter $\delta = \delta_J + \delta_\beta \approx \delta_J$ owing to the fact that δ_β is at least three orders of magnitude less that δ_J (see Equation (19)). The parameter $\epsilon \ll 1$ and it is therefore natural to consider the expansion $\tilde{u}_p = \tilde{u}_p^{(0)} + \epsilon\tilde{u}_p^{(1)} + O(\epsilon^2)$. Substituting this expansion in (20) and (21) yields to leading order

$$\delta\tilde{u}_p^{(0)\prime\prime} = \tilde{f}_p^{(0)}\tilde{u}_p^{(0)2} \,, \tag{22}$$

subject to

$$\tilde{u}_p^{(0)}(0) = -1, \quad \tilde{u}_p^{(0)}(1) = 0 \,. \tag{23}$$

This result shows that, to leading order, liquid inertia effects can be neglected in long wells. The model as defined by Equations (22) and (23) is the original model of Dikken [3]. Note that Dikken's model does not include inertia effects which our analysis shows to be a valid approximation for the case of long wells. However, in the next section it will be shown that under special circumstances inertia effects have to be included. For the case in which the Blasius correlation is used (see Equation (6)) the friction factor $\tilde{f}_p$ is a nonlinear function of $\tilde{u}_p$ ($\tilde{f}_p \sim \tilde{u}^{1/4}$). For that case we are not aware of an analytical solution of (22) subject to the boundary conditions (23). For the case in which $\tilde{f}_p$ is taken to be a constant, independent of $\tilde{u}_p$, it turns out that (22)–(23) has an analytical solution in terms of a Weierstrass elliptic function (see Halvorsen [4]).

It is not necessary to solve (22)–(23) in order to determine some of the main solution characteristics. Note, first of all, that the right-hand side of (22) is strictly positive, implying that $\tilde{u}_p$ is a strictly increasing, convex function. The characteristics of this convex function will clearly depend on the magnitude of the parameter δ. In the case where $\delta \gg 1$ we can write $\tilde{u}_p^{0)} = \tilde{u}_{p,0}^{(0)} + \delta^{-1}\tilde{u}_{p,1}^{(0)} + O(\delta^{-2})$, which on substituting in (22) yields to leading order the linear solution

$$\tilde{u}_{p,0}^{(0)} = \tilde{x} - 1 \,. \tag{24}$$

The physical interpretation of this solution is that, in the case where the reservoir permeability is low, the frictional pressure losses in the well are small compared with the differential pressure required to extract oil from the reservoir. Thus, the difference in pressure between the well and the reservoir is, to leading order, constant along the length of the well. This result is obtained immediately by substituting the leading-order solution (24) in (18) to yield $\Delta\tilde{p} = \delta + O(1)$. This implies that there is a uniform production of oil along the total length of the well - the ideal situation! Note that this result can always be achieved by making the well sufficiently short.

In the case where $\delta \ll 1$ it is evident that the solution of (22) has a boundary layer character. A regular perturbation expansion of $\tilde{u}_p$ in terms of δ yields immediately that $\tilde{u}_p^{(0)} = 0 + O(\delta)$ in the outer region. To find the solution in the inner (boundary-layer) region we stretch the $\tilde{x}$ coordinate via $\hat{x} = \tilde{x}/\sqrt{\delta}$ and consider the expansion $\tilde{u}_p = \hat{u}_p + O(\delta)$. To leading order, this yields

$$\hat{u}_p'' = \hat{f}_p \hat{u}_p^2 \tag{25}$$

subject to the boundary conditions

$$\hat{u}_p(0) = -1 \quad \text{and} \quad \hat{u}_p(\infty) \to 0 \,. \tag{26}$$

The second of the above boundary conditions follows from the solution $\tilde{u}_p^{(0)} = 0$ in the outer region. If the Blasius correlation as given in Section 2 and the dimensionless form of $\hat{f}_p$ as in (14) are applied, it follows that $\hat{f}_p = \frac{1}{2}|\hat{u}_p|^{-1/4}$. Using this form for the friction factor we find that Equation (25), subject to the given boundary conditions, has the solution

$$\hat{u}_p = -\left[34\sqrt{11}\hat{x} + 1\right]^{-8/3} \,. \tag{27}$$

The above solution was also found by Dikken [3] in his limit of infinitely long wells. Equation (27) shows a rapid decline of the velocity magnitude as one moves towards the toe of the

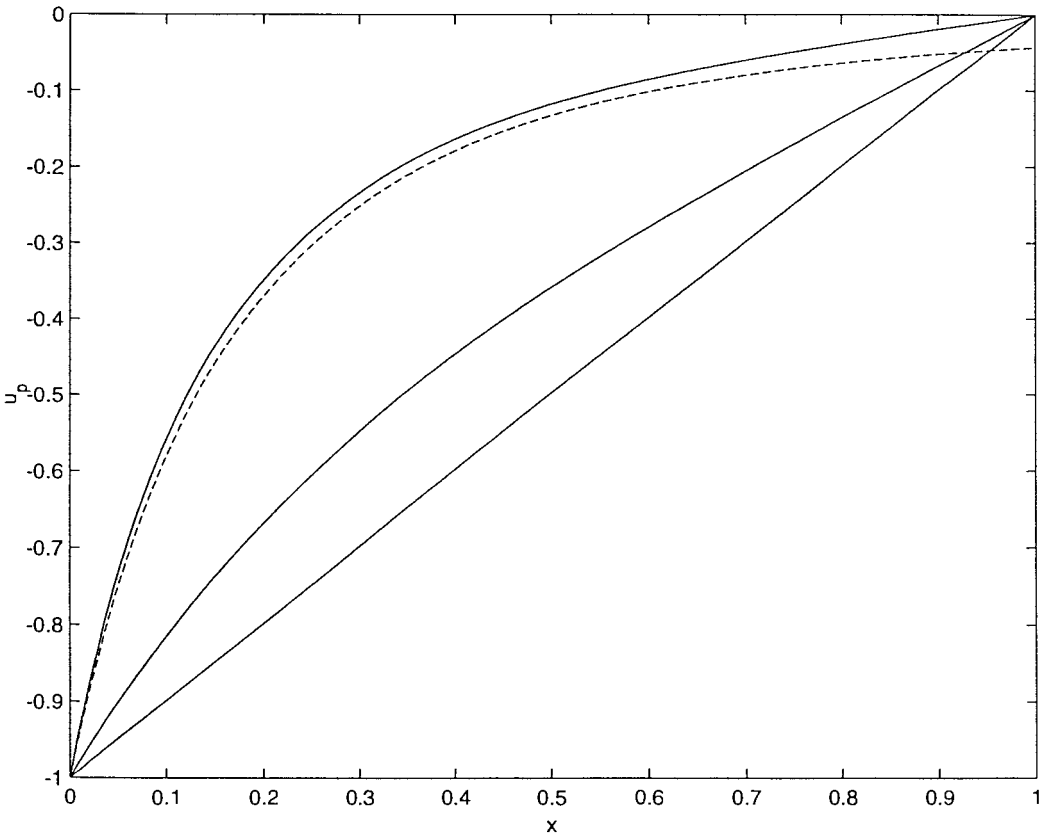

Figure 2. The solution characteristics of Equation (20) for the values $\delta = 10^{-2}$, $\delta = 10^{-1}$, and $\delta = 10$ as indicated in the plot. The dashed line shows the asymptotic solution (27) for the case in which $\delta = 10^{-2}$.

well. As expected, this decline in the velocity magnitude is matched by a rapidly diminishing differential pressure between the well and the reservoir. Substitution of (27) in (18) shows that in the heel of the well the differential pressure $\Delta\tilde{p} = O(\delta)$; it decreases rapidly to a magnitude of order $\Delta\tilde{p} = O(\delta^{17/6})$ as one moves towards the toe of the well. The results obtained here for the case in which $\delta \ll 1$ show that the effective production length of the well is of order $\sqrt{\delta}$. At distances $\gg \sqrt{\delta}$ from the heel of the well, the difference in pressure between the reservoir and the well has decreased so much that very little oil is extracted from the reservoir.

Figure 2 summarises the results of the analysis given above. In the figure we show the computed velocity profiles along the length of the well for the cases $\delta = 10^{-2}$, $\delta = 10^{-1}$, and $\delta = 10$. The dashed line shows the asymptotic solution (27) for the case in which $\delta = 10^{-2}$.

3.2. Flow in the well and the annulus: case $\delta_J \gg 1$

The analysis in the previous section shows that, in the case where there is no flow m the annulus, the solution properties are mainly determined by the parameter δ_J: in the case where $\delta_J \gg 1$ the velocity is a linear function (to leading order) of the position along the length of the well, while in the case $\delta_J \ll 1$ the solution has a boundary-layer character. As will be shown in this section, there are additional boundary layers present when flow in the annulus is included. In order to simplify the analysis we start with the assumption that $\delta_J \gg 1$ such that

the new boundary layer becomes more transparent. The equations which will be analysed are (15)–(17) and we consider the regular expansions

$$\tilde{u}_p = u_p^{(0)} + \delta_J^{-1} u_p^{(1)} + \cdots ,$$
$$\tilde{u}_a = u_a^{(0)} + \delta_J^{-1} u_a^{(1)} + \cdots .$$

On substituting the above expansions in (15)–(17) we obtain at leading order

$$\begin{aligned} O(0):\ & u_p^{(0)\prime\prime} + r_A u_a^{(0)\prime\prime} = 0 , \\ & u_p^{(0)\prime\prime} + r_A u_a^{(0)\prime\prime} = 0 , \\ & u_p^{(0)}(0) = -1, u_p^{(0)}(1) = u_a^{(0)}(0) = u_a^{(0)}(1) = 0 \end{aligned} \tag{28}$$

and at first order

$$\begin{aligned} O(\delta_J^{-1}):\ & u_p^{(1)\prime\prime} + r_A u_a^{(1)\prime\prime} + \delta_\beta u_p^{(0)\prime\prime} - (2-\lambda)\epsilon u_p^{(0)} u_p^{(0)\prime} = f_p^{(0)} u_p^{(0)2} , \\ & u_p^{(1)\prime\prime} + r_A u_a^{(1)\prime\prime} - (2-\lambda)\epsilon u_a^{(0)} u_a^{(0)\prime} = f_a^{(0)} u_a^{(0)2} , \\ & u_p^{(1)}(0) = u_p^{(1)}(1) = u_a^{(1)}(0) = u_a^{(1)}(1) = 0 , \end{aligned} \tag{29}$$

in which $f_p^{(0)} = \tilde{f}_p(u_p^{(0)})$ and likewise for $f_a^{(0)}$. Note that at leading order we obtain two identical equations which can be solved subject to the boundary conditions to yield

$$u_p^{(0)} + r_A u_a^{(0)} = \tilde{x} - 1 . \tag{30}$$

Evidently, in the case where $\delta_J \gg 1$ we retain a linear velocity profile but now for the weighted sum of the velocities in the annulus and the base pipe (Equation (30) states, in fact, that the total volume flow rate in base pipe and annulus varies linearly with $\tilde{x}$). Note that the leading-order problem is not solved by Equation (30) alone, since we do not know individual velocity profiles in the base pipe and the annulus. In order to obtain the individual velocity profiles we have to consider the first-order equations given in (29). There we can see that the first-order terms in both equations are identical. Thus, on subtracting the second differential equation in (29) from the first, we obtain an equation which contains only zeroth-order quantities. Proceeding in this manner and making the substitution $\delta_\beta = \epsilon\alpha$, we obtain

$$\begin{aligned} & \epsilon\alpha u_p^{(0)\prime\prime} - (2-\lambda)\epsilon u_p^{(0)} u_p^{(0)\prime} + (2-\lambda)\epsilon u_a^{(0)} u_a^{(0)\prime} = f_p^{(0)} u_p^{(0)2} - f_a^{(0)} u_p^{(0)2} , \\ & u_p^{(0)} + r_A u_p^{(0)} = \tilde{x} - 1 , \\ & u_p^{(0)}(0) = -1, u_p^{(0)}(1) = u_a^{(0)} = u_a^{(0)}(1) = 0 . \end{aligned} \tag{31}$$

The new parameter $\alpha = A_p/\beta\rho LU = O(10^{-3})$ is the ratio of pressure forces required to get fluid through the sand screen and inertia forces. We are now in a position to consider the expansions

$$\begin{aligned} u_p^{(0)} &= u_{p,0} + \epsilon u_{p,1} + \cdots , \\ u_a^{(0)} &= u_{a,0} + \epsilon u_{a,1} + \cdots . \end{aligned} \tag{32}$$

Using (32) in (31) we obtain the following equations at leading order

$$\begin{aligned} & f_{a,0} u_{a,0}^2 = f_{p,0} u_{p,0}^2 , \\ & u_{p,0} + r_A u_{a,0} = \tilde{x} - 1 , \\ & u_{p,0}(0) = -1, u_{p,0}(1) = u_{a,0}(0) = u_{a,0}(1) = 0 , \end{aligned} \tag{33}$$

in which $f_{p,0} = f_p^{(0)}(u_{p,0})$ and likewise for $f_{a,0}$. The first of the equations in (33) is essentially a statement of the fact that the pressure gradients in the annulus and the base pipe are, to leading order, the same. In other words, the difference in pressure between the annulus and the base pipe is of order $O(\epsilon^2)$. The solution of the equations specified in (33) is clearly determined by the forms of the friction factors in the base pipe and the annulus. For simplicity we consider the case in which the flow is turbulent in both the annulus and the base pipe, assuming a concentric arrangement of the base pipe in the annulus. With these assumptions one obtains the following values for the parameters in the friction factor as define by Equation (6): $a_p = 0{\cdot}316$, $b_p = 0{\cdot}25$ for the base pipe and $a_a = 0{\cdot}35$, $b_a = 0{\cdot}25$ for the annulus. With these expressions for the fraction factors we find that the first equation in (33) yields $u_{p,0} = \sigma u_{a,0}$ in which $\sigma = \left(\frac{0{\cdot}35}{0{\cdot}316}\right)^{4/7} \left(\frac{D_p}{D_a - D_0}\right)^{5/7}$. This result together with the second of the equations in (33) yields then

$$\begin{aligned} u_{p,0} &= \frac{\sigma}{\sigma + r_A}(\tilde{x} - 1) \ , \\ u_{a,0} &= \frac{1}{\sigma + r_A}(\tilde{x} - 1) \ . \end{aligned} \tag{34}$$

The solutions as given in (34) reveal a linear velocity profile along the length of both the well in both the base pipe and the annular cavity. Note that the boundary conditions for both the base pipe and annulus velocities are satisfied at $\tilde{x} = 1$. However, at $\tilde{x} = 0$ neither of the solutions as given in (34) satisfy the imposed boundary conditions. This indicates that solution found in (34) represents the outer solution and further work is required to find the correct behaviour inside the boundary layer. Recall that in the case where no flow in the annulus was present, no solution with boundary-layer characteristics was found for the case with $\delta_J \gg 1$ as is being considered here. Evidently, a new boundary layer is obtained by including flow in the annulus.

In order to study the solution of (31) inside the boundary layer we stretch the $\tilde{x}$-co-ordinate via $\bar{x} = \tilde{x}/\alpha$ and we consider the expansions

$$\begin{aligned} u_p^{(0)} &= \bar{u}_p + O(\alpha) \ , \\ u_a^{(0)} &= \bar{u}_a + O(\alpha) \ . \end{aligned} \tag{35}$$

Substituting the expansions (35) in (31) and applying the co-ordinate stretching as given above, we find that at leading order, $O(\epsilon/\alpha)$, the following equations are obtained

$$\begin{aligned} &\bar{u}_p'' - (2 - \lambda)\bar{u}_p\bar{u}_p' + (2 - \lambda)\bar{u}_a\bar{u}_a' = 0 \ , \\ &\bar{u}_p + r_A\bar{u}_a = -1 \ , \\ &\bar{u}_p(0) = -1 \ , \\ &\bar{u}_a(0) = 0 \ , \end{aligned} \tag{36}$$

subject to the matching conditions

$$\bar{u}_p(\infty) = u_p^O \ , \quad \bar{u}_a(\infty) = u_a^O \ . \tag{37}$$

Clearly, the matching conditions depend on the flow conditions in the annulus. In the case where we have turbulent flow in the annulus, application of (34) yields $u_p^O = -\dfrac{\sigma}{\sigma + r_A}$ and

$u_a^O = \dfrac{-1}{\sigma + r_A}$. The differential equation in (36) can be integrated once and the second equation in (36) can subsequently be used to eliminate $\bar{u}_a$ from the equations. The resulting first-order differential equation in $\bar{u}_p$ can be integrated, which, on applying the boundary conditions as given in (36) and the matching conditions (37), yields

$$\begin{aligned} \bar{u}_p(\bar{x}) &= \frac{1}{2a}\left[b - \frac{c\tanh(c\bar{x}/2) + b + 2a}{1 + \frac{b+2a}{c}\tanh(c\bar{x}/2)} \right], \\ \bar{u}_a(\bar{x}) &= -\frac{1}{r_a}(1 + \bar{u}_p(\bar{x})), \end{aligned} \tag{38}$$

in which $a = (1 - \lambda/2)(1 - 1/r_A^2)$, $b = (2 - \lambda)/r_A^2$ and $c = b - 2au_p^O$. The results so far indicate that, in the case where flow in the annulus is included, a new boundary layer appears which has a thickness $O(\alpha)$. The physical interpretation of the results is as follows. In most of the well (the outer region) fluid in the annulus flows towards the heel of the well maintaining the same pressure gradient in the annulus as in the base pipe. At a distance $O(\alpha)$ upstream from the end of the annulus, the fluid in the annulus begins to notice the blockage at the heel. Over a distance $O(\alpha)$ the fluid in the annulus is decelerated. The decrease in inertia of the fluid in the annulus leads to pressure build-up in the annulus which subsequently forces the annular fluid through the sand screen and into the base pipe. Figure 3 shows the shape of the analytical solution as given by Equations (34) and (38). We have taken $\alpha = 10^{-2}$ for the case shown.

Before we proceed to study the case in which $\delta_J \ll 1$ it is interesting to investigate how the reservoir 'feels' the presence of the well. Equation (3) describes the flow rate from the reservoir into the well. In dimensionless form this equation reads

$$\tilde{w} = \tilde{u}_p' + r_A\tilde{u}_a', \tag{39}$$

where $\tilde{w} = \pi D_a w/A_p U$ is the dimensionless flow rate from the reservoir into the well. From Equations (30) and (39) we find that $\tilde{w} = 1$ along the whole length of the well. This result implies that in the case $\delta_J \gg 1$, that is a low-permeability reservoir, the well is seen by the reservoir as a line source of constant strength. The rapid changes of the well flow in the boundary layer as described by Equations (38) do therefore not propagate into the reservoir. The reason for this is that the ratio $\delta_{\beta/\delta_J} \ll 1$.

3.3. Flow in the well and the annulus: case $\delta_J \ll 1$

Going back to the analysis for the case with no annulus is present, we recall that the production profile had boundary layer characteristics when $\delta_J \ll 1$. The thickness of the boundary layer was found to be of order $O(\sqrt{\delta_J})$. The analysis in the previous section showed that with the presence of the annulus, a boundary layer with a thickness $O(\alpha)$ appears. Therefore, in the case where we assume that an open annulus is present in a well in a high-permeability reservoir (that is $\delta_J \ll 1$), we expect two boundary layers to appear: a 'thick' reservoir-induced boundary layer with a thickness $O(\sqrt{\delta_J})$ and a 'thin' annulus-induced boundary layer with a thickness $O(\alpha)$. In what follows, the details of these boundary-layer solutions are exposed.

Given that $\delta_J \ll 1$, we consider the regular expansions

$$\begin{aligned} \tilde{u}_p &= u_p^{(0)} + \delta_J u_p^{(1)} + \cdots, \\ \tilde{u}_a &= u_a^{(0)} + \delta_J u_a^{(1)} + \cdots. \end{aligned}$$

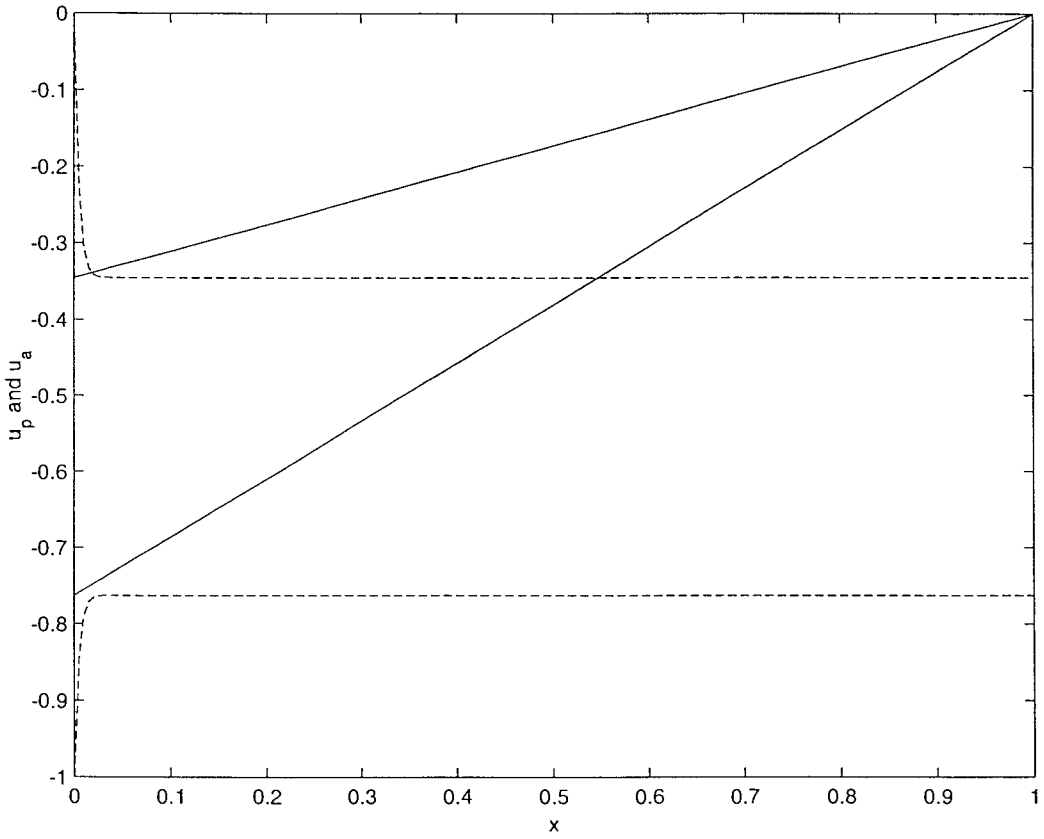

Figure 3. The matched asymptotic solution as given by Equations (34) and (38) for the case in which $\alpha = 10^{-2}$. The solid lines denote outer solutions as given in (34), while the dashed line denote the inner solutions as defined in (38).

On substituting the above expansions in (15)–(17) we obtain at leading order

$$\begin{aligned} f_p^{(0)} u_p^{(0)2} &= 0\,, \\ f_a^{(0)} u_a^{(0)2} &= 0\,. \end{aligned} \tag{40}$$

These equations have solutions $u_p^{(0)} = u_a^{(0)} = 0$ which satisfy the boundary conditions at $\tilde{x} = 1$ but not the boundary conditions at $\tilde{x} = 0$. Clearly this represents the outer solution and further analysis is required in order to find the inner solution. We now introduce the a boundary-layer co-ordinate $\hat{x} = \tilde{x}/\sqrt{\delta_J}$. In terms of this stretched co-ordinate Equations (15)–(16) can be written in the form

$$\begin{aligned} &\frac{\epsilon\alpha}{\delta_J}\hat{u}_p'' - (2-\lambda)\frac{\epsilon}{\delta_J}\hat{u}_p\hat{u}_p' + (2-\lambda)\frac{\epsilon}{\delta_J}\hat{u}_a\hat{u}_a' = \hat{f}_p\hat{u}_p^2 - \hat{f}_a\hat{u}_a^2, \\ &\hat{u}_p'' + r_A\hat{u}_a'' - (2-\lambda)\frac{\epsilon}{\delta_J}\hat{u}_a\hat{u}_a' = \hat{f}_a\hat{u}_a^2, \end{aligned} \tag{41}$$

subject to the boundary conditions $\hat{u}_p(0) = -1$, $\hat{u}_a(0) = 0$ and the matching conditions $\hat{u}_p = \hat{u}_a = 0$ as $\hat{x} \to \infty$. Note that, as in the previous section, we have made the substitution $\delta_\beta = \epsilon\alpha$. Next, we consider the regular expansions

$$\begin{aligned} \hat{u}_p &= \hat{u}_p^{(0)} + O(\epsilon/\sqrt{\delta}) \,, \\ \hat{u}_a &= \hat{u}_a^{(0)} + O(\epsilon/\sqrt{\delta}) \,, \end{aligned} \tag{42}$$

which, on substitution in (41), yields at leading order

$$\begin{aligned} &\hat{f}_{p,0}\hat{u}_p^{(0)2} - \hat{f}_{a,0}\hat{u}_a^{(0)2} = 0 \\ &\hat{u}_p^{(0)\prime\prime} + r_A\hat{u}_a^{(0)\prime\prime} = \hat{f}_{a,0}\hat{u}_a^{(0)_2} \,, \end{aligned} \tag{43}$$

subject to the matching conditions $\hat{u}_p^{(0)} = \hat{u}_a^{(0)} = 0$ as $\hat{x} \to \infty$. The above equations do not uniquely define $\hat{u}_p^{(0)}$ and $\hat{u}_a^{(0)}$, since the equations are not independent. This is a similar situation to what was found in the previous section where the case $\delta_J \gg 1$ was considered. Solving the Equations in (43) we have

$$\begin{aligned} \hat{u}_p^{(0)} &= -\left(34\sqrt{\frac{A}{11}}\hat{x} + C\right)^{-8/3} \,, \\ \hat{u}_a^{(0)} &= \frac{1}{\sigma}\hat{u}_p^{(0)} \,, \end{aligned} \tag{44}$$

in which $A = \sigma/(\sigma + r_A)$, where σ as defined previously and C is an, as yet, undetermined constant. Note that the solution as given above satisfies the boundary conditions at $\hat{x} \to \infty$, but the conditions in the heel of the well at $\hat{x} = 0$ are still not satisfied. The solution given by Equations (44) represent the 'thick' reservoir-induced boundary layer. In order to satisfy the boundary conditions in the heel of the well the solution in the 'thin' annulus-induced boundary layer needs to be found. Considering Equations (41) we clearly see that the solution in the thin boundary layer is obtained when we balance the terms on the left-hand side of the first equation in (41). This balance is obtained when the x-co-ordinate is stretched according to $\bar{x} = \hat{x}/(/\sqrt{\delta_J})$. Introducing this co-ordinate stretching in (41) and considering the expansion

$$\begin{aligned} \hat{u}_p^{(0)} &= \bar{u}_p + O(\alpha/\sqrt{\delta_J}) \,, \\ \hat{u}_a^{(0)} &= \bar{u}_a + O(\alpha/\sqrt{\delta_J}) \,, \end{aligned} \tag{45}$$

we obtain at leading order

$$\begin{aligned} &\bar{u}_p'' - (2-\lambda)\bar{u}_p\bar{u}_p' + (2-\lambda)\bar{u}_a\bar{u}_a' = 0 \,, \\ &\bar{u}_p'' + r_A\bar{u}_a'' = 0 \,, \\ &\bar{u}_p(0) = -1 \,, \\ &\bar{u}_a(0) = 0 \,, \end{aligned} \tag{46}$$

subject to the matching conditions

$$\bar{u}_p(\infty) = \hat{u}_p^{(0)}(0) = -C^{-8/3}, \quad \bar{u}_a(\infty) = \hat{u}_p^{(0)}(0) = -\frac{1}{\sigma}C^{-8/3} \,. \tag{47}$$

From the second equation in (46), together with the boundary conditions at $\bar{x} = 0$ and the requirement that both $\bar{u}_p$ and $\bar{u}_a$ remain bounded as $\bar{x} \to \infty$, we obtain immediately that $\bar{u}_p + r_A\bar{u}_a = -1$. This result, together with the matching conditions as specified in (47), yields $C = (1 + r_A/\sigma)^{3/8}$.

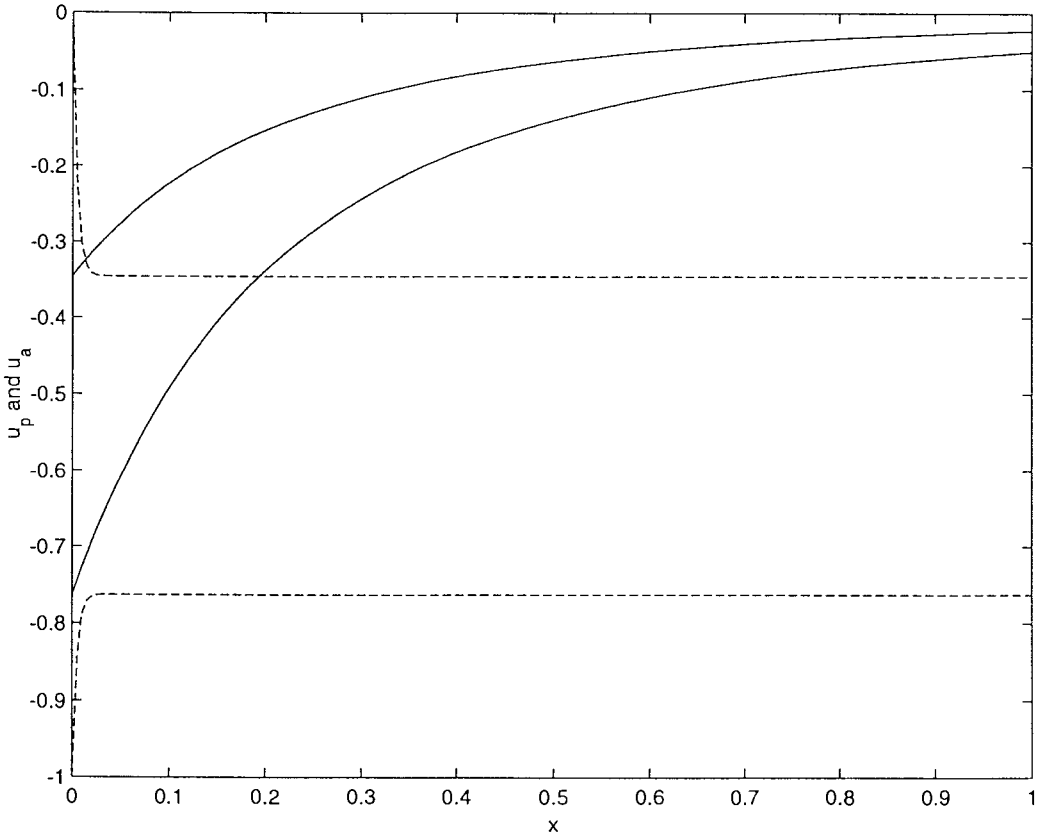

Figure 4. The matched asymptotic solution as given by Equations (44) and (48) for the case in which $\alpha = 10^{-2}$ and $\delta_J = 10^{-2}$. The drawn lines denote outer solutions as given in (44), while the dashed lines denote the inner solutions as defined in (48).

As a check on the analysis so far we consider the limit where $r_A \to 0$, which is a vanishing annulus cross section. In this limit $\sigma \to \infty$, so that $C \to 1$. Going back to Equations (44) we see that in this limit $A \to 1$, $\hat{u}_a^{(0)} \to 0$ and $\hat{u}_p^{(0)}$ attains the required form as found earlier in the analysis for the case without the presence of the annulus (*cf.* Equation (27)).

Going back to Equations (46) we note that these equations are identical to those found in the previous section (*cf.* Equations (36)). This indicates that, as expected, the structure in the thin boundary layer is unaltered by the reservoir conditions, that is, the parameter δ_J. We note also that the thickness of the thin boundary layer is the same as in the previous section, namely $O(\alpha)$. The equations in (46) subject to the boundary and matching conditions can, as before, be integrated to yield

$$\begin{aligned} \bar{u}_p(\bar{x}) &= \frac{1}{2a}\left[b - \frac{c\tanh(c\bar{x}/2) + b + 2a}{1 + \frac{b+2a}{c}\tanh(c\bar{x}/2)} \right], \\ \bar{u}_a(\bar{x}) &= -\frac{1}{r_A}(1 + \bar{u}_p(\bar{x})), \end{aligned} \tag{48}$$

in which $a = (1 - \lambda/2)(1 - 1/r_A^2)$, $b = (2 - \lambda)/r_A^2$ and $c = b + 2a(1 + r_A/\sigma)^{3/8}$. Figure 4 shows the shape of the analytical solution as given by Equations (44) and (48). We have taken $\alpha = 10^{-2}$ and $\delta_J = 10^{-2}$ for the case shown.

We now investigate how the reservoir feels the presence of the well. In the previous section it was shown that the dimensionless flow rate from the reservoir into the well, namely $\tilde{w}$, is given by Equation (39). Using the results given in Equations (44) and (46), we obtain

$$\tilde{w} = 2\sqrt{\frac{A}{11}}(1+\frac{1}{\sigma})\left(\frac{3}{4}\sqrt{\frac{A}{11}}\frac{\tilde{x}}{\sqrt{\delta_J}}+C\right)^{-11/3} . \tag{49}$$

As in the case with $\delta_J \gg 1$, the details in the thin, annulus-induced boundary layer are not seen by the reservoir. However, the above equation show clearly that the flow rate from the reservoir into the well decreases rapidly for increasing $\tilde{x}$. Thus, reservoir experiences the well as a sink with a rapidly decreasing strength as one moves from the heel to the toe of the well.

4. Numerical solutions

In what follows numerical solutions of the dimensionless equivalents of Equations (9)–(12) will be presented. We will be satisfied with outlining the method and procedure which are used to solve the coupled nonlinear equations without going into the details of the numerical solution algorithm. Applying a standard finite-element procedure (using linear basis functions) to the differential Equations (9)–(10) we obtain the coupled systems of equations

$$(S_\beta + S_J)\mathbf{u}_p + S_J\mathbf{u}_a + C_p(\mathbf{u}_p)\mathbf{u}_p = F_p(\mathbf{u}_p)\mathbf{u}_p + \mathbf{r}_p \ , \tag{50}$$

$$S_J\mathbf{u}_p + S_J\mathbf{u}_a + C_a(\mathbf{u}_a)\mathbf{u}_a = F_a(\mathbf{u}_a)\mathbf{u}_a + \mathbf{r}_a \ . \tag{51}$$

The relation between the discrete systems of equations as given above and Equations (9)–(10) is as follows. The stiffness matrices S_J and S_β are related to the second-order derivatives, the convective matrices $C_p(\mathbf{u}_p)$ and $C_a(\mathbf{u}_a)$ are related to the first-order derivatives and the friction matrices $F_p(\mathbf{u}_p)$ and $F_a(\mathbf{u}_a)$ are related to the friction factor terms. The vectors $\mathbf{r}_p$ and $\mathbf{r}_a$ contain terms related to the boundary conditions. Assume that we have some initial guesses $\mathbf{u}_p^{(0)}$ and $\mathbf{u}_a^{(0)}$ of the solution vectors $\mathbf{u}_p$ and $\mathbf{u}_a$. The nonlinear system of equations is now solved iteratively as follows. We first take (50)-$\mu\times$ (51) where $0 < \mu \leq 1$. The resulting system is then used to find an update of the approximation of $\mathbf{u}_p$ via

$$\begin{aligned}[S_\beta + (1-\mu)S_j + C_p(\mathbf{u}_p^{(n)}) - F_p(\mathbf{u}_p^{(n)})]\mathbf{u}_p^{(n+1)} &= \mathbf{r}_p - \mu\mathbf{r}_a \ , \\ -[(1-\mu)S_J + \mu C_a(\mathbf{u}_a^{(n)}) + \mu F_a(\mathbf{u}_a^{(n)})]\mathbf{u}_a^{(n)} &\end{aligned} \tag{52}$$

and a new estimate of $\mathbf{u}_a$ is obtained from

$$[S_J + C_a(\mathbf{u}_a^{(n)}) - F_a(\mathbf{u}_a^{(n)})]\mathbf{u}_a^{(n+1)} = \mathbf{r}_a - S_J\mathbf{u}_p^{n+1)} \ . \tag{53}$$

The reason for subtracting the multiple of (51) from (50) is related to the boundary-layer character of the solution. Taking $\mu = 0$ we find that the iteration procedure is robust but the boundary layer is not resolved properly. Taking $\mu = 1$ we obtain an iterative procedure which has a small radius of convergence but it gives a good resolution of the boundary layer. The iterative procedure (52)–(53) is continued until convergence is attained. In the numerical computations 400 elements are used to discretise the interval [0, 1].

The analysis presented in the previous section is based on the assumption that $\delta_J \gg 1$. This assumption leads to the result that the total volume flow rate in the base pipe and annulus

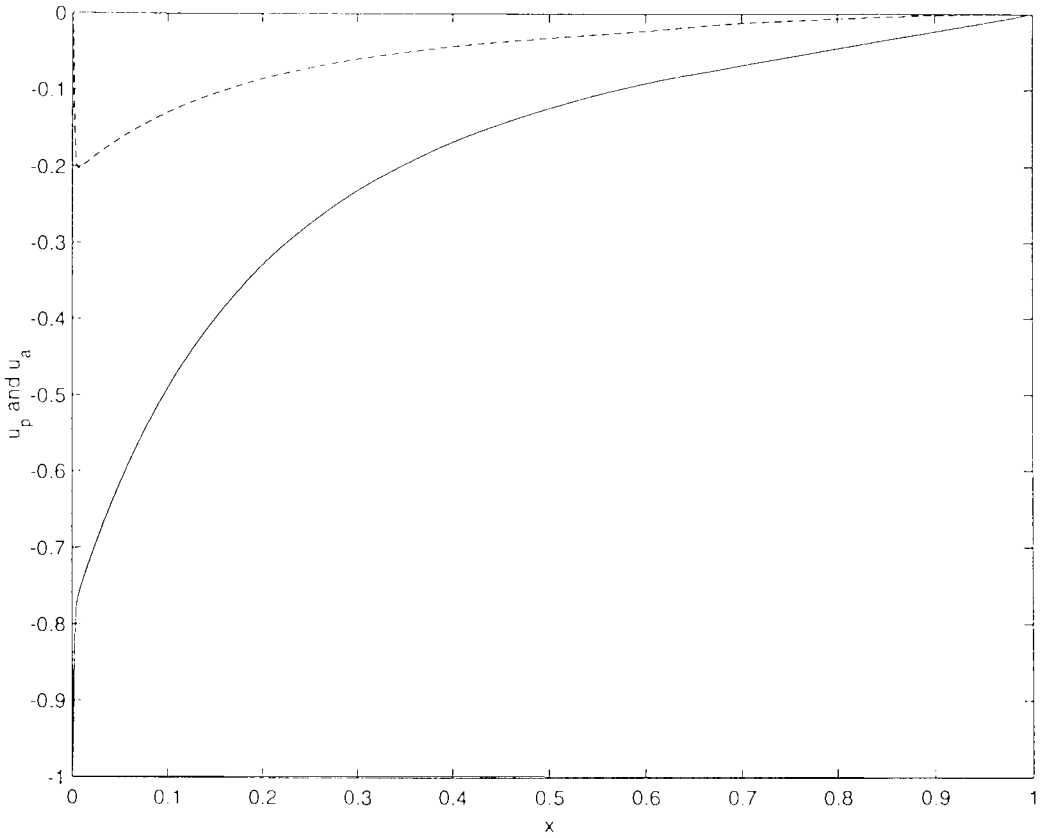

Figure 5. Plots of the numerical solution of Equations (15)–(17) for the parameter values $\alpha = 10^{-2}$ and $\delta_J = 10^{-2}$ (a), $\delta_J = 0{\cdot}1$ (b) and $\delta_J = 10$ (c). The drawn lines denotes the base pipe velocity $u_p(x)$, while the dashed lines denotes the annulus velocity $u_a(x)$.

decreases linearly from the heel to the toe of the well. In Section 3.1 it was shown that the velocity profile along the length of the well will also exhibit boundary-layer behaviour in the case where $\delta_J \ll 1$. This boundary layer results when long wells are drilled in high permeability reservoirs. The thickness of this 'reservoir-induced' boundary layer was shown to be of order $\sqrt{\delta}$. Combining the results of the analysis presented in Sections 3.1 and 3.2 we come to the conclusion that in a well where there is possibility for flow in the annulus and the base pipe, one may find two distinct boundary layers. There may be a reservoir-induced boundary layer with a thickness of order $\sqrt{\delta_J}$ and an 'annulus-induced' boundary layer with a thickness of order α. Referring to (19), where the orders of magnitude of the dimensionless groups are listed, together with the definition of $\alpha = \delta_\beta/\epsilon$, we find that the annulus-induced boundary layer is approximately two orders of magnitude thinner than the reservoir-induced boundary layer.

Figures 5a–c show the computed velocity profiles for the case in which $r_A = 0{\cdot}75$, $\epsilon = 10^{-2}$, $\alpha = 10^{-3}$ and $\delta_J = 10^{-2}$ (a), $\delta_J = 0{\cdot}1$ (b) and $\delta_J = 10$ (c), respectively.

The thin, annulus-induced boundary is evident in all figures, while the reservoir-induced boundary layer becomes apparent in Figure 5(a).

One interesting property of the annulus-induced boundary layer is the fact that it occurs whenever there is a change in the cross sectional area of the annulus. To exemplify this we

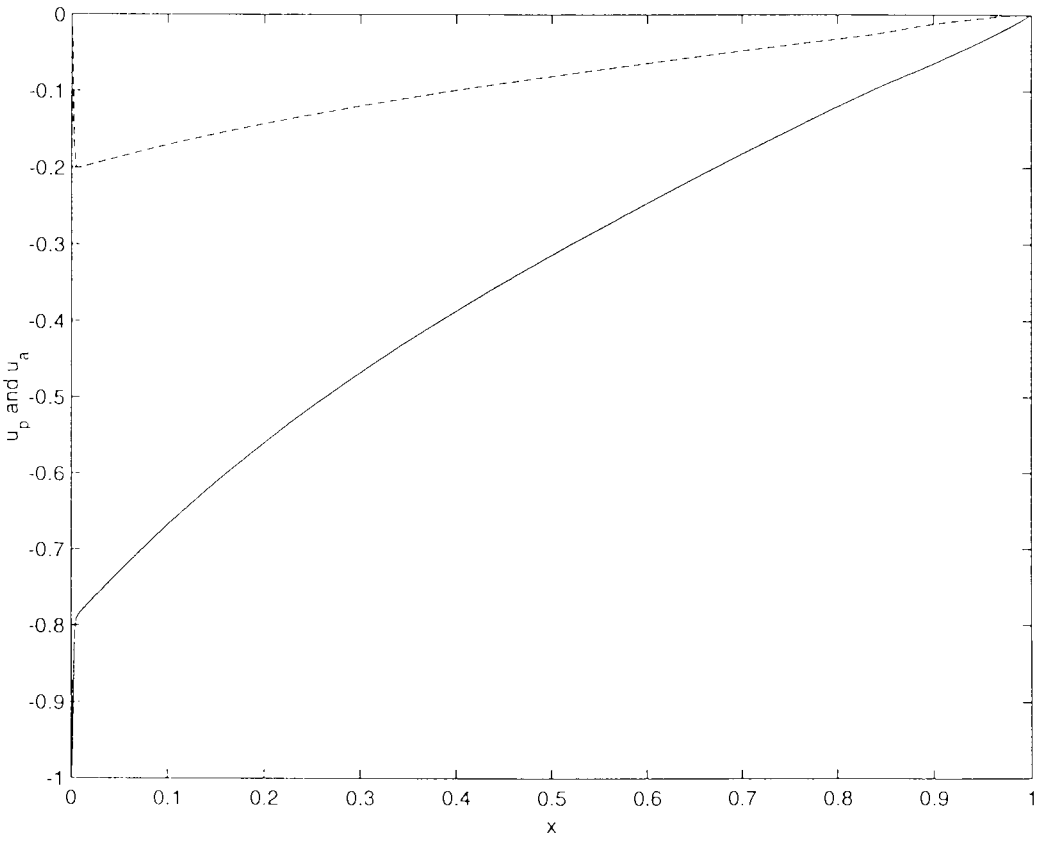

Figure 5. Continued.

consider the following variation in r_A. In the intervals $\tilde{x} \in [0, 0{\cdot}2] \cup [0{\cdot}3, 0{\cdot}35]$ we assume an open annulus with $r_A = 0{\cdot}75$, while in the remainder of the interval [0,1] we reduce the annulus area such that $r_A = 0{\cdot}1$. Figure 6 shows the computed velocity profiles for the base pipe and the annulus. The presence of a change in the degree of openness of the annulus is thus reflected in an abrupt change in the fluid velocity in the base pipe.

This is a result of significant practical value. Namely, while it is possible to measure the flow in the base pipe of an actual well, it is not possible to determine the flow in the annulus by direct measurements. Our analysis indicates that abrupt changes in the base-pipe velocity over a length scale of order $O(\alpha)$ are a definite signature of the presence of flow in the annulus. Flow in the annulus can thus be inferred from variations in the measured flow in the base pipe.

In what follows some measurements will be discussed which show that the results of the foregoing analysis do, in fact, reflect phenomena observed in actual oil-production wells. Figure 7 shows the measured velocity profile in a production well which, at the time when the measurement was taken, produced only oil (a light crude with a viscosity somewhat less than 2cP). The total length of the weil was approximately 1350m and the reservoir in which the well was drilled had a high permeability. For this case the dimensionless reservoir parameter $\delta_J \approx 0{\cdot}06$. This particular well was almost horizontal with maximal deviations from the horizontal plane of less than 2m. The measurements are obtained by inserting a long string into the well with at the end of the string a spindle which measures the local fluid velocity.

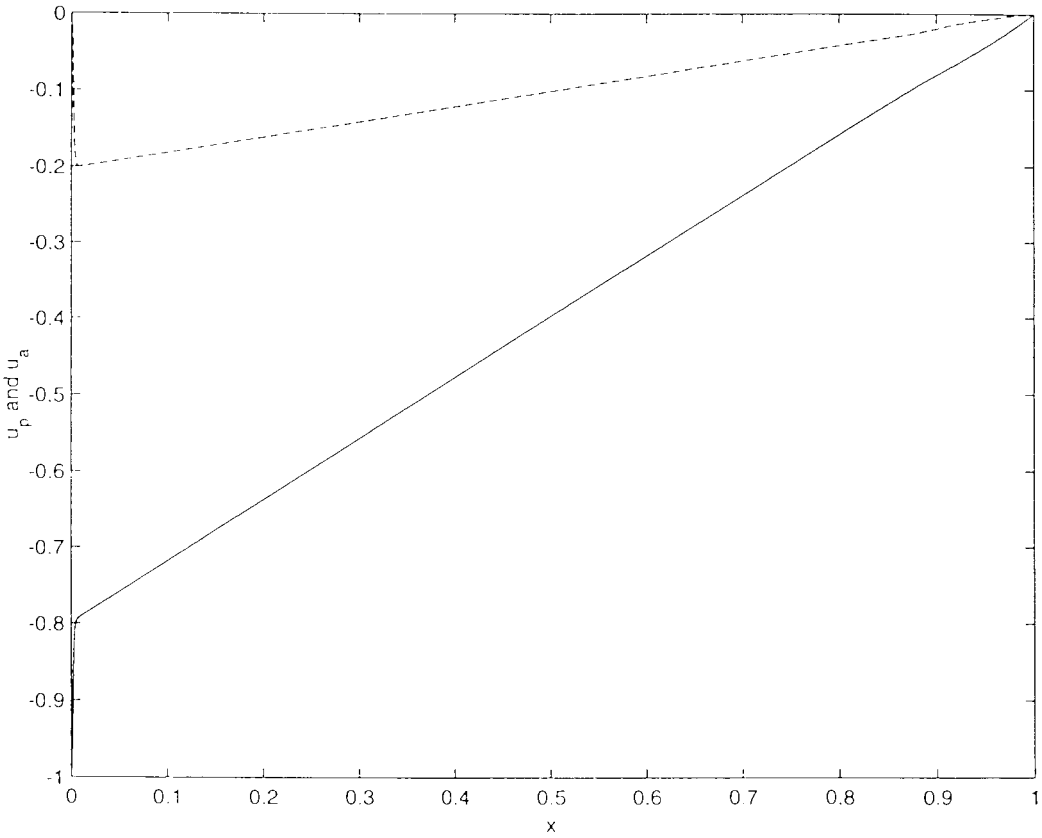

Figure 5. Continued.

One of the most striking features in the measured velocity in Figure 7 is the very sharp decrease in the velocity magnitude in the heel of the well. A comparison of Figures 7 and 5(a) shows a very similar qualitative behaviour. This suggests that the rapid change in the measured velocity as seen in Figure 7 is due to annulus fluid entering the base pipe in the heel of the well. It is in principle possible that, by coincidence, the heel of the well is situated in a region of the reservoir with a very high permeability, giving rise to the observed jump in the measured velocity. However, if one computes the permeability required to give a jump of a kind as seen in Figure 7, one finds that this permeability would have to be four orders of magnitude larger than the known mean reservoir permeability. It is unlikely that this is the case. In addition to the large change in the velocity magnitude near the heel of the well, Figure 7 also shows an abrupt decrease in the measured velocity at a distance of approximately 250m from the heel of the well. Also in this case, the length scale over which the change in the velocity occurs is such that it can only be attributed to the presence of flow in the annulus at the position of the sudden decrease *cf.* Figure 6. Geological information, in fact, supports this interpretation. Measurements show that at the position where the velocity decreases, there is a calcite formation in the reservoir which otherwise consists mainly of sandstone. The calcite is hard rock at which collapse of the bore hole is very unlikely, in contrast to most of the rest of the reservoir.

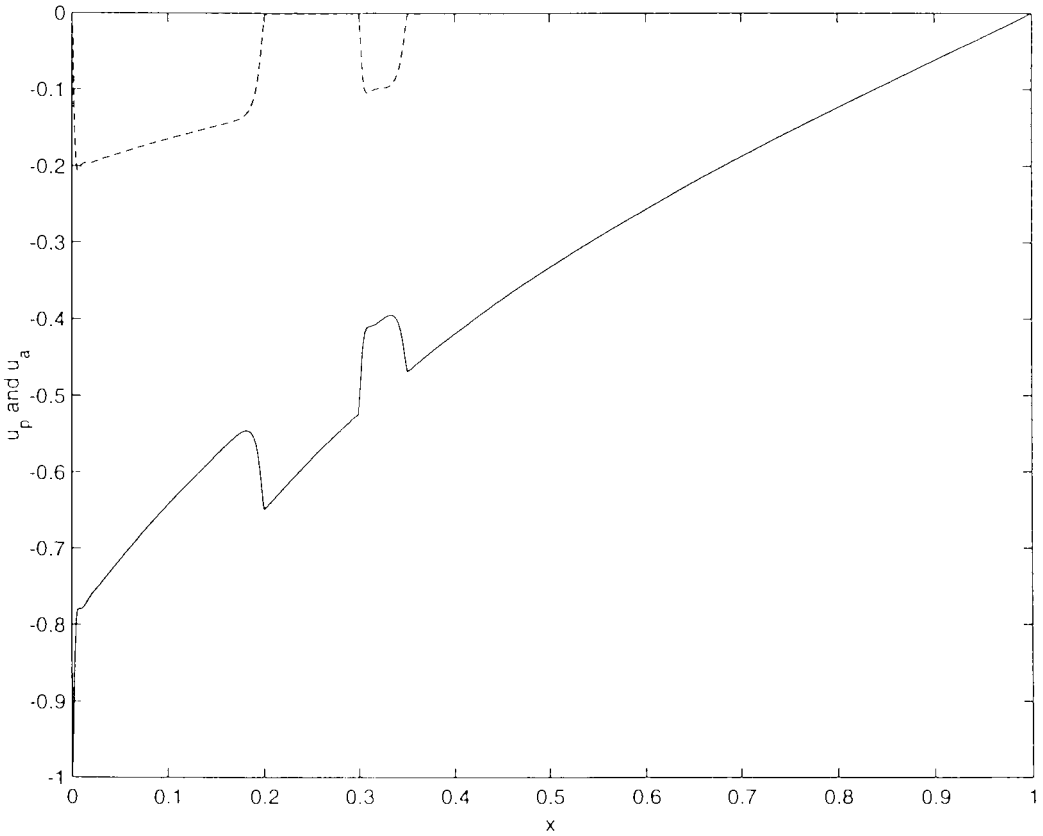

Figure 6. Plot of the computed velocity profiles in the base pipe (solid line) and annulus (dashed line) for the case in which the annulus has a varying cross-sectional area.

5. Conclusions

In this paper we have presented a hydraulic model for the flow in a horizontal well. The model allows for flow in an annulus outside the main flow pipe (the 'base pipe') as well as for flow inside the base pipe. Two nonlinear coupled ODE's are obtained which are analysed in this paper. First of all, a simplified case is studied which is obtained by letting the area of the annulus vanish such that only flow in the base pipe needs to be considered. Analysis of this simplified case shows that the solution of the governing equation may have a boundary layer in the heel of the well. This boundary layer results when a sufficiently long well is drilled in a high-permeability reservoir. This is what we call a 'reservoir-induced' boundary layer. In this case the pressure drop in the base pipe is of the same order of magnitude as the pressure difference between the well and the reservoir. This results in the oil being produced only locally (near the heel) while in most of the well the pressure difference between the well and the reservoir is too small to extract significant quantities of oil from the reservoir. When the well is drilled in a reservoir with a very low permeability, the production profile decreases linearly from the heel to the toe of the well.

When flow in the annulus is taken into account a new boundary layer is found. This boundary layer is the result of fluid flowing in the annulus being forced into the base pipe when the annulus becomes blocked. The length over which the annular fluid flows into the

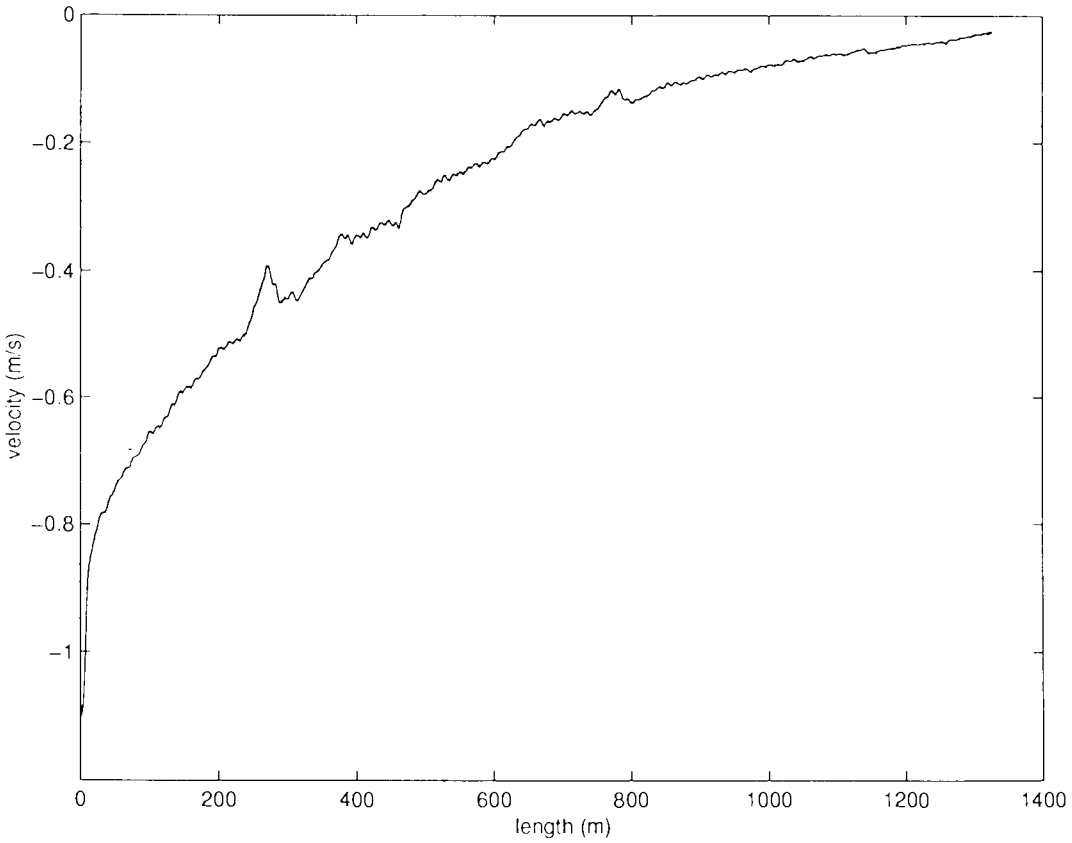

Figure 7. Plot showing the measured velocity profile in an actual production well.

base pipe is small. It is governed by the balance of deceleration forces and pressure forces required to press fluid into the base pipe. The new boundary layer is an 'annulus-induced' boundary layer since it results from the change of the geometry of the annulus. For typical parameters it is shown that the thickness of the reservoir-induced boundary layer is at least two orders magnitude larger than the geometry-induced boundary layer.

Acknowledgements

We are indebted to Norsk Hydro for giving us permission to publish this work.

References

1. G. C. Hocking and L. K. Forbes, Super-critical withdrawl from a two-layer fluid through a line sink if the lower layer is of finite depth. *J. Fluid Mech.* 428 (2001) 333–348.
2. S. D. Joshi, *Horizontal Well Technology*. Tulsa: PennWell Publishing Company (1991) 535 pp.
3. B. J. Dikken, Pressure drop in horizontal wells and its effect on production performance. *J. Petrol. Techn.* (1990) 1426–1433.
4. G. Halvorsen, Discussion of Considering wellbore friction effects in planning horizontal wells. *J. Petrol. Techn.* (1994) 620.
5. L. B. Ouyang, Single phase and multi-phase fluid flow in horizontal wells. *PhD Thesis, Dept. of Petrol. Engng.* Stanford University (1998).

6. R. M Olsen and E. R. G. Eckert, Experimental studies of turbulent flow in a porous circular tube with uniform injection through the tube wall *ASME J. Appl. Mech.* (1966) 7–17.
7. R. M. S. M. Schulkes, T. Rinde and O.H. Utvik, Pipe flow with radial inflow: experimental and modelling work. *J. Fluids Engng.* 121 (1999) 106–111.
8. V. K. Jonsson and E. M. Sparrow, Experiments on turbulent-flow phenomena in eccentric annular ducts. *J. Fluid Mech.* 25 (1966) 65–86.
9. I. E. Idelchik (ed.) *Handbook of Hydraulic Resistance.*
10. M. Golan and C. H. Whitson, *Well Performance*. Englewood Cliffs: New York: Bepell Press (1996) 790 pp. Prentice Hall (1991).